General Disclaimer

One or more of the Following Statements may affect this Document

- This document has been reproduced from the best copy furnished by the organizational source. It is being released in the interest of making available as much information as possible.

- This document may contain data, which exceeds the sheet parameters. It was furnished in this condition by the organizational source and is the best copy available.

- This document may contain tone-on-tone or color graphs, charts and/or pictures, which have been reproduced in black and white.

- This document is paginated as submitted by the original source.

- Portions of this document are not fully legible due to the historical nature of some of the material. However, it is the best reproduction available from the original submission.

NASA TECHNICAL
MEMORANDUM

NASA TM X-73362

A LONG-LIVED CORONAL X-RAY ARCADE

By J. P. McGuire, E. Tandberg-Hanssen, K. R. Krall,
S. T. Wu, J. B. Smith, Jr., and D. M. Speich
Space Sciences Laboratory

January 1977

NASA

George C. Marshall Space Flight Center
Marshall Space Flight Center, Alabama

TECHNICAL REPORT STANDARD TITLE PAGE

1. REPORT NO. NASA TM X-73362	2. GOVERNMENT ACCESSION NO.	3. RECIPIENT'S CATALOG NO.
4. TITLE AND SUBTITLE A Long-Lived Coronal X-Ray Arcade		5. REPORT DATE January 1977
		6. PERFORMING ORGANIZATION CODE
7. AUTHOR(S) J. P. McGuire, E. Tandberg-Hanssen, K. R. Krall,* S. T. Wu,* J. B. Smith, Jr.,** and D. M. Speich**		8. PERFORMING ORGANIZATION REPORT #
9. PERFORMING ORGANIZATION NAME AND ADDRESS George C. Marshall Space Flight Center Marshall Space Flight Center, Alabama 35812		10. WORK UNIT, NO.
		11. CONTRACT OR GRANT NO.
		13. TYPE OF REPORT & PERIOD COVERED
12. SPONSORING AGENCY NAME AND ADDRESS National Aeronautics and Space Administration Washington, D.C. 20546		Technical Memorandum
		14. SPONSORING AGENCY CODE

15. SUPPLEMENTARY NOTES
Prepared by Space Sciences Laboratory, Science and Engineering
*Affiliated with The University of Alabama in Huntsville, Huntsville, Alabama
**Affiliated with NOAA; presently at the Marshall Space Flight Center

16. ABSTRACT

A large, long-lived, soft X-ray emitting arch system was observed during the last Skylab mission. This arcade of arches stayed in the same approximate position for several solar rotations. This report suggests that these long-lived arches owe their stability to the stable coronal magnetic-field configuration. A global constant α force-free magnetic field analysis, as developed by Nakagawa et al., is used to describe the arches, and a marked resemblance is noted between the theoretical magnetic-field configuration and the observed X-ray emitting feature.

17. KEY WORDS	18. DISTRIBUTION STATEMENT Unclassified — Unlimited C. P. McGuire

19. SECURITY CLASSIF. (of this report) Unclassified	20. SECURITY CLASSIF. (of this page) Unclassified	21. NO. OF PAGES 24	22. PRICE NTIS

MSFC - Form 3292 (Rev December 1972) For sale by National Technical Information Service, Springfield, Virginia 22151

TABLE OF CONTENTS

Page

LIST OF ILLUSTRATIONS

A LONG-LIVED CORONAL X-RAY ARCADE

I. INTRODUCTION

One of the outstanding realizations to follow from analyses of the Skylab/
Apollo Telescope Mount data is that the Sun's atmosphere is considerably more
dynamic than had hitherto been assumed. Although it has been known for years
that abrupt changes take place in coronal structures in response to disturbances
from below, the extent and frequency of such coronal transients are much
greater than previously known. However, while these findings are very impor-
tant for our understanding of the physics of the solar atmosphere, we also find
that at times parts of the corona remain virtually unchanged for long periods
of time.

One of the best ways to study these long-lived coronal shapes is to
record their X-ray emission. Since the coronal structures are dictated by
magnetic fields, important information also can be extracted on these long-
lived coronal magnetic fields by analyzing coronal shapes as revealed in X-rays.

Large coronal arches had been observed prior to the Skylab mission;
Dunn [1] found that the λ 5303, FeXIV emission, as recorded by a ground-
based coronagraph, revealed arches reaching altitudes greater than 0.5 solar
radii above the limb. The purpose of this report is to present the results of
an analysis of a particularly well-observed, long-lived coronal arch system
during the Skylab mission.

II. OBSERVATIONS

Both the X-ray telescopes of the Marshall Space Flight Center/The
Aerospace Corporation and of American Science and Engineering observed the
arches in question.

The arcade structure was a very faint and relatively cool feature. The Marshall Space Flight Center/The Aerospace Corporation telescope observed the feature with filters that had a transmission range from 8 to 20 Å (harder filters). The arches appeared bright enough to be studied on the film but were too faint to be successfully reproduced photographically. The American Science and Engineering telescope observed with a softer filter which transmitted in the wavebands 2 to 32 Å and 44 to 54Å, making photographic reproduction possible in this case. However, the telescope during this time period had its shutter blade misaligned, producing a linear image of the blade and resulting in appreciable X-ray scattering. More detailed descriptions of the telescopes have been written by Underwood, et al. [2] and Vaiana, et al. [3]. On December 26, 1973, the structure appeared on the western limb as shown in Figure 1a. Figure 1b depicts the features as seen through the harder filters, while Figure 1c shows the locations of the active regions, the positions of the coronal holes, and the position of the arcade. Figure 1d presents the appearance of the white-light corona, as observed with the High Altitude Observatory K-coronameter. In early January, the arches were seen as they came over the eastern limb (Fig. 2). Figure 3 shows the area over which the arches were located as it appeared on the disk in mid-January. The arcade had its footpoints along the southern border of the active regions; i.e., from approximately 160 to 280 degrees longitude. The area of interest is bounded by a coronal hole and by active regions. The arch structures cannot be clearly distinguished in this picture because the arcade structure is seen clearly only in projection against the dark sky background. During the latter part of January, the arcade was again on the western limb (Fig. 4). The operation of Skylab then ceased before the structure could reappear on the eastern limb.

The structure, composed of an arcade of arches, outlines particular coronal magnetic flux tubes which run basically in a north-south direction. The flux tubes reach heights of 0.7 $R_\odot$ above the limb and have footpoint separations as great as 50 heliographic degrees. As noted in the Introduction, Dunn observed structures of a similar size and shape in λ 5303. However, these structures connected active regions. The longest arches interconnecting active regions, observed by the X-ray instruments onboard Skylab, had footpoint separations of no more than 37 degrees [4]. The large arches analyzed in this report connected active region areas and coronal hole boundaries.
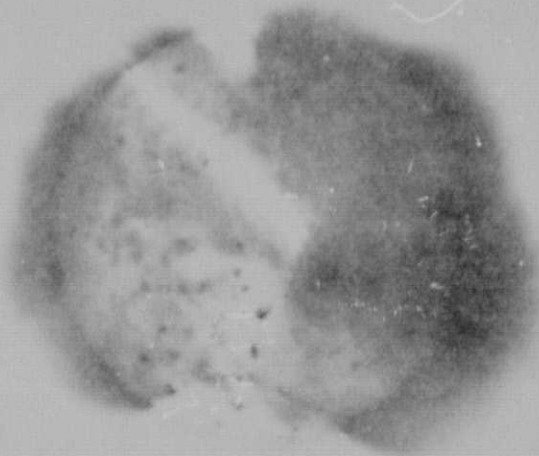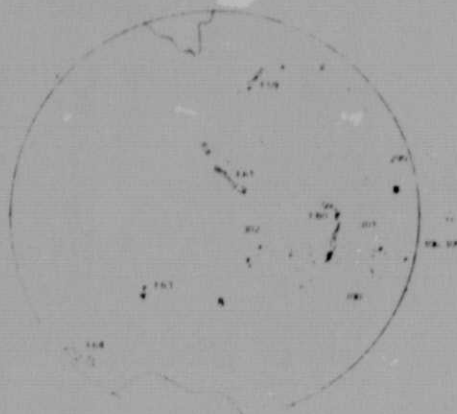
a. X-ray photograph showing the arch on the western limb
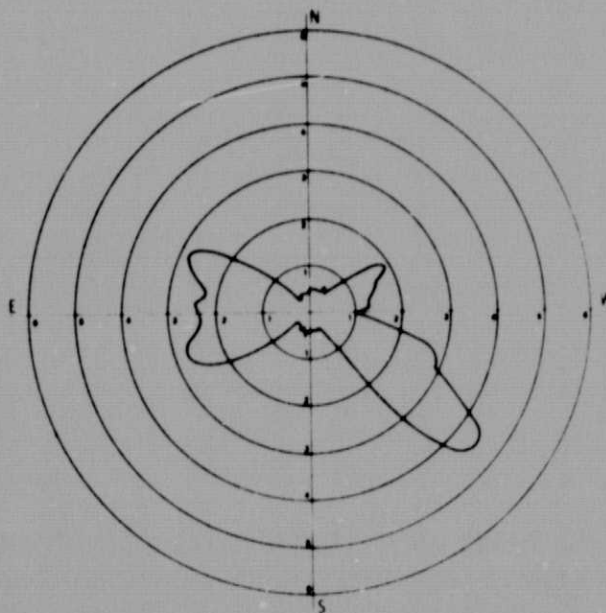(courtesy American Science and Engineering).
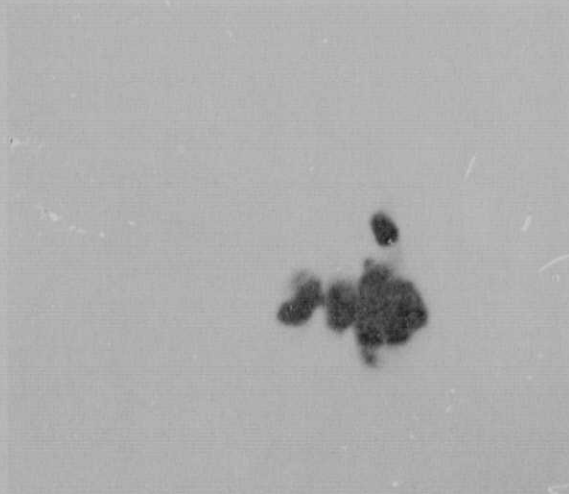
b. X-ray photograph showing the active regions lining the
northern feet of the arcade (Marshall Space Flight Center/
The Aerospace Corporation); the active regions are
composed of numerous narrow flux tubes not resolved
in the reproduction.

Figure 1.   Observations of the long-lived southern arch system on
December 26, 1973.

c. "Neutral line drawing" showing the locations of the
features of interest; the hatched-in areas are
coronal holes and the location of the arch is indicated.

d. K-coronameter intensity plot (courtesy High Altitude
Observatory. Note: Observations pertain to a distance of
$1/2\ R_\odot$ (solar radius) above the limb, and the intensity is
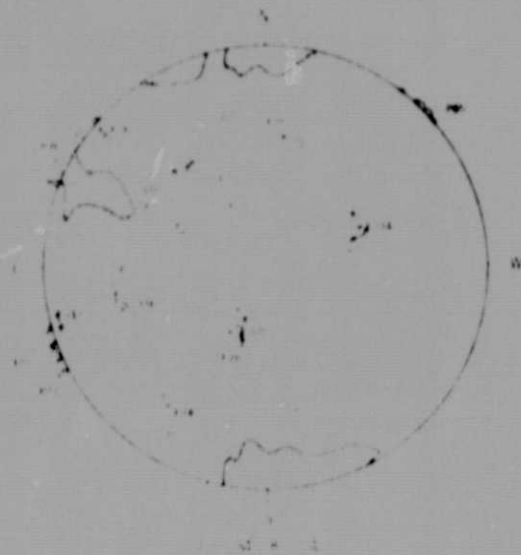proportional to the radial distance from the Sun center.)

Figure 1. (Concluded).
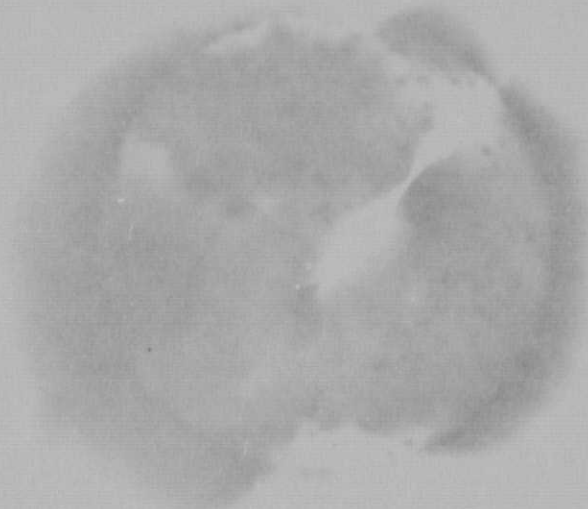
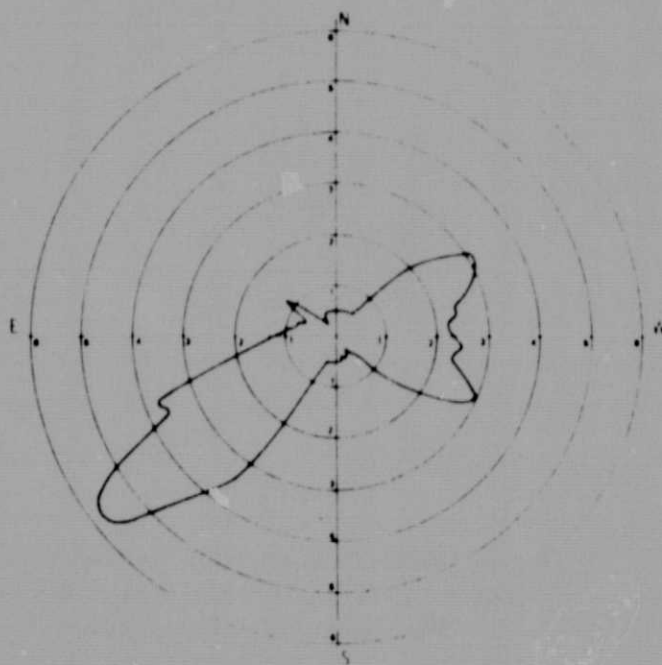a. X-ray photograph showing the arcade on the southeastern limb (courtesy American Science and Engineering).
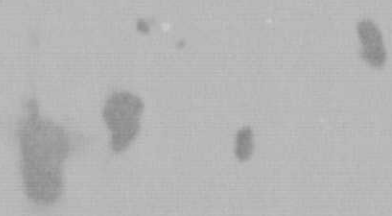
b. X-ray photograph showing the associated active regions (Marshall Space Flight Center/ The Aerospace Corporation).

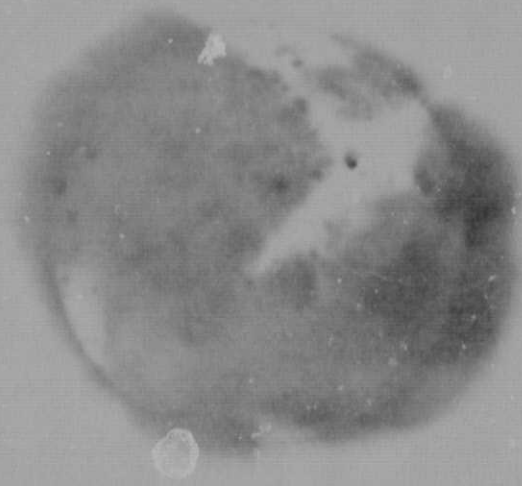Figure 2. Observations of the arcade on January 11, 1974.

c. "Neutral line drawing" showing the locations of the features of interest.
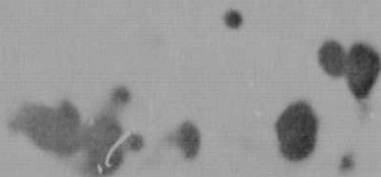

d. K-coronameter intensity plot (courtesy High Altitude Observatory), compare Figure 1.

Figure 2. (Concluded).

a. Faint-feature X-ray photograph (courtesy American Science and Engineering).

b. Bright-feature photograph (Marshall Space Flight Center/ The Aerospace Corporation).

Figure 3. The solar disk on January 18, 1974, showing the location of the arcade.

$L_0 \cdot 199^\circ,\ B_0 \cdot 4.85^\circ$

c. "Neutral line drawing."
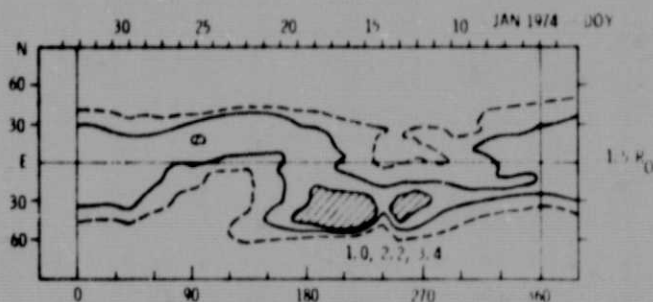
d. K-coronameter intensity map for the January time period (courtesy High Altitude Observatory); the arcade is in the southern hemisphere from approximately 160 to 280 degrees longitude.
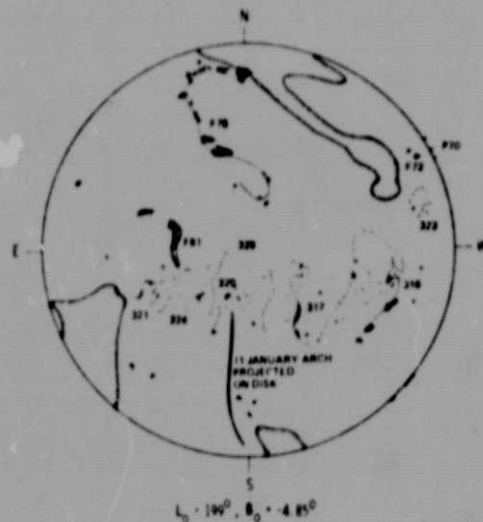
Figure 3. (Concluded).
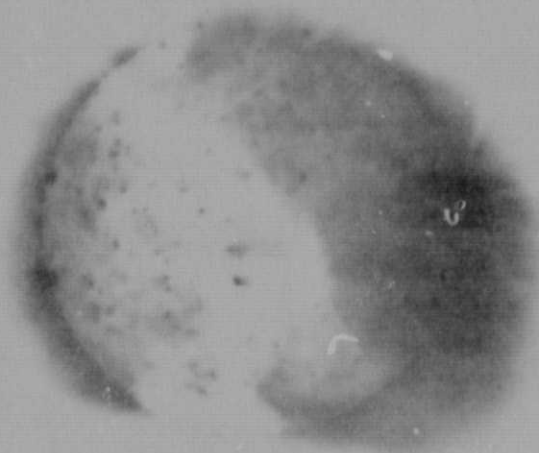
a. Faint-feature X-ray photograph (courtesy American Science and Engineering).

b. Bright-feature photograph (Marshall Space Flight Center/The Aerospace Corporation).

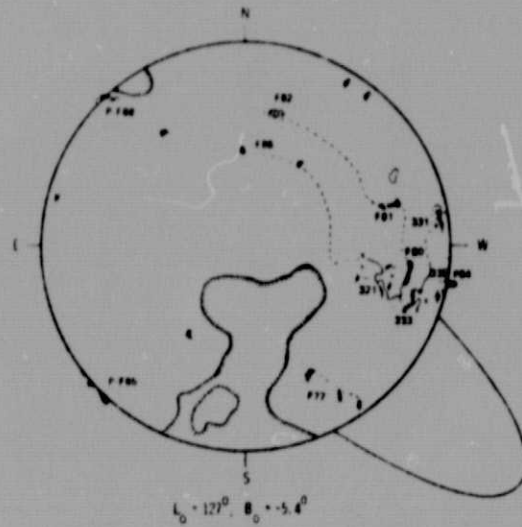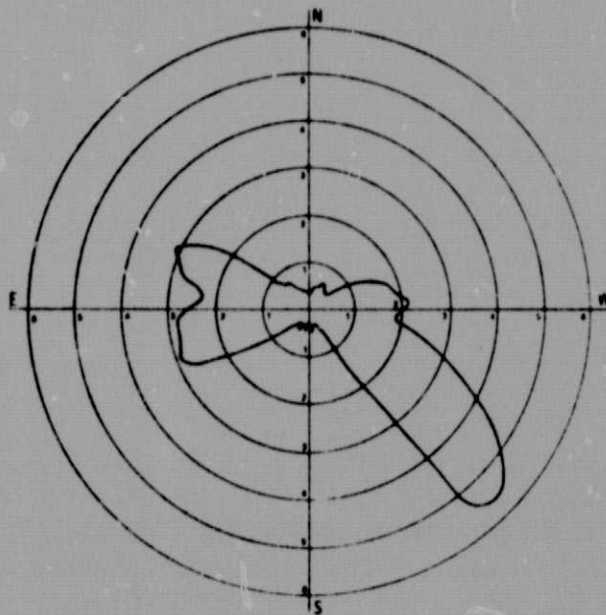Figure 4. Observations of the arch system on the western limb on January 23, 1974.

$L_0 = 127°, B_0 = -5.4°$

c. "Neutral line drawing."

d. K-coronameter intensity plot (courtesy High Altitude Observatory), compare Figure 1.

Figure 4. (Concluded).

III. REPRESENTATION OF GLOBAL MAGNETIC FIELDS

We wish to represent one of the stable arches as seen on the limb in December and January in terms of a global force-free magnetic-field configuration. Representing a magnetic field as the curl of a vector potential A_ϕ, we write in spherical coordinates

$$B = \left[\frac{1}{r^2 \sin \theta} \frac{\partial}{\partial \theta} (r A_\phi \sin \theta) \ , \ -\frac{1}{r \sin \theta} \frac{\partial}{\partial r} (A_\phi r \sin \theta) \ , \ B_\phi \right] \tag{1}$$

Following Nakagawa et al. [5], we apply the force-free condition

$$\nabla \times B = \alpha B \quad , \tag{2}$$

where we chose α constant along a field line and in time to simplify the problem. A constant α is not a strong physical requirement to obtain long-lasting structure. Under conditions in a static corona, resistive diffusion will cause field deformation of a nonconstant α force-free field in a time $t \sim (n\alpha^2)^{-1}$ (n = resistivity) much greater than the observed arch lifetime.

The general solution becomes

$$A(r,\mu) = \sum_{n=1}^{\infty} A_n P_n^{1}(\mu) \frac{J_{-n-1/2}(\alpha r)}{r^{1/2}} \quad |\alpha| > 0 \tag{3a}$$

$$A^*(r,\mu) = \sum_{n=1}^{\infty} A_n^* P_n^{1}(\mu) \frac{1}{r^{n+1}} \quad , \quad \alpha = 0 \tag{3b}$$

where $P_n(\mu)$ is the Legendre function of degree n and argument $\mu = \cos\theta$, and $J_{-n-1/2}$ is the Bessel function of order $-(n+1/2)$. In the potential field case ($\alpha = 0$, denoted by *), the solution with $r^{-(n+1)}$ is chosen to insure convergence for $r \to \infty$. Using equations (3a) and (3b), we may write equation (1) in the form

$$B_r = \sum_{n=1}^{\infty} n(n+1)\, A_n P_n(\mu) \left(\frac{R}{r}\right)^{3/2} \frac{J_{-n-1/2}(\alpha r)}{J_{-n-1/2}(\alpha R)} \quad , \quad \alpha \neq 0$$

$$= \sum_{n=1}^{\infty} n(n+1) A_n^* P_n(\mu) \left(\frac{R}{r}\right)^{n+2} \quad , \quad \alpha = 0$$

(4a)

$$B_\theta = \sum_{n=1}^{\infty} A_n P_n^1(\mu) \quad n\left(\frac{R}{r}\right)^{3/2} \frac{J_{-n-1/2}(\alpha r)}{J_{-n-1/2}(\alpha R)}$$

$$+ \alpha R\left(\frac{R}{r}\right)^{1/2} \frac{J_{-n-1/2}(\alpha r)}{J_{-n-1/2}(\alpha R)} \quad , \quad \alpha \neq 0$$

(4b)

$$= \sum_{n=1}^{\infty} n A_n^* P_n^1(\mu)\left(\frac{R}{r}\right)^{n+2} \quad , \quad \alpha = 0$$

$$B_\phi = \sum_{n=1}^{\infty} A_n P_n^1(\mu)\left(\frac{R}{r}\right)^{1/2} (\alpha R) \frac{J_{-n-1/2}(\alpha r)}{J_{-n-1/2}(\alpha R)} \quad , \quad \alpha \neq 0$$

(4c)

$$= 0 \quad , \quad \alpha = 0$$

where A_n and A_n^* have been redefined in terms of the surface value of B_r (i.e., at $r = R_\odot$, where $R_\odot$ is the solar radius).

The projection of the coronal arch on the observing plane (the $r - \theta$ plane) will satisfy

$$\frac{dr}{B_r} = \frac{r d\theta}{B_\theta} \quad , \tag{5}$$

or $rA \sin \theta = C$ (constant). Therefore, we may write

$$C = \sum_{n=1}^{\infty} A_n^* \sin \theta \, P_n^1(\mu) f(r) \quad ,$$

where

$$f(r) = R^2 \left(\frac{r}{R}\right)^{1/2} \frac{J_{-n-1/2}(\alpha r)}{J_{-n-1/2}(\alpha R)} \quad , \quad \alpha \neq 0 \quad ,$$

and

$$f(r) = R^2 \left(\frac{R}{r}\right)^n \quad , \quad \alpha = 0 \quad ,$$

or, upon expanding,

$$C = A_1 \sin^2 \theta \, f(r) + A_2 [3 \sin^2 \theta \cos \theta] f(r)$$
$$+ A_3 \left[\frac{3}{2} \sin^2 \theta (5 \cos^2 \theta - 1)\right] f(r) + \ldots \ldots \quad . \tag{6}$$

We choose to represent the arch with a one-term quadruple approximation ($n = 2$), with constants combined, and have

$$C^1 = r^{1/2} \sin^2 \theta \cos \theta \, J_{-5/2}(\alpha r) \quad , \quad \alpha \neq 0$$

$$= r^{-2} \sin^2 \theta \cos \theta \quad . \quad , \quad \alpha = 0 \quad . \tag{7}$$

Using a maximum height $r \approx 1.5$ to $1.7 \, R_\odot$ and the approximate footpoint positions previously given, we find good agreement with the observed structure for $|\alpha| \leq 1.5/R_\odot$ ($2.1 \times 10^{-11} \, \mathrm{cm}^{-1}$).

For a given choice of the parameters r_{max} and α, equation (7) can be used to determine C^1. This in turn defines the shape of the arch and, in particular, the distance between footpoints. Figure 5 shows a comparison between the observed field structure as seen in X-rays and a few of a series of generated arch configurations for two values of r_{max}. An increase in α causes flattening of the projected arch and a corresponding widening of the distance between footpoints. Relatively good agreement is found when $|\alpha| \lesssim 1.3 \, R_\odot^{-1}$, while values above $1.5 \, R_\odot^{-1}$ show marked departure from observations. Any inclination of the plane of the arch to the local meridian will produce projection effects, causing a "high α" limb arch to appear more "potential" when seen projected on the observing plane. We find that a difference of 10 degrees in heliographic longitude of the footpoints produces no appreciable error in α-estimation, while 25 degrees would be needed to give rather serious degenerations in true arch shapes. There is a strong likelihood, therefore, that no significant error is introduced to the upper limit set on the magnitude of α.

We may estimate the current density J within a magnetic system by using equation (2) in the form

$$\vec{\nabla} \times \vec{B} = \alpha \vec{B} = \mu_0 \vec{J} \quad ,$$
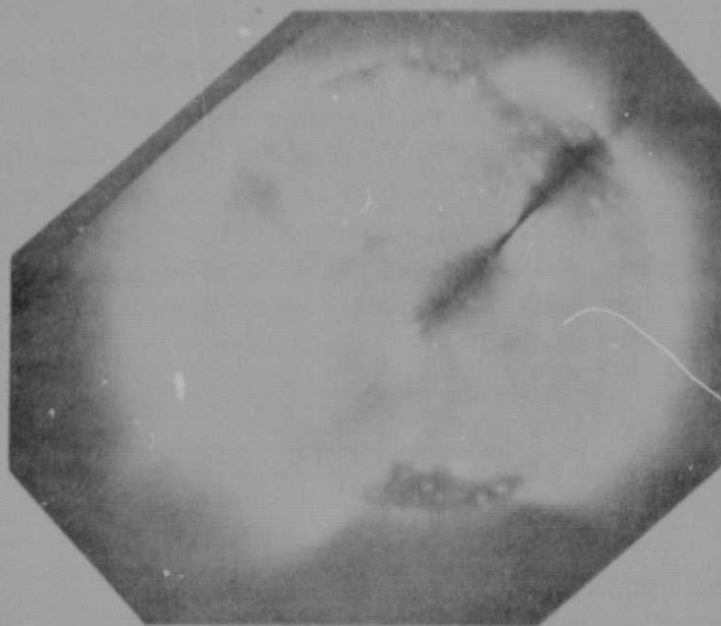
a. January 11, 1974, X-ray photograph (courtesy American Science and Engineering).
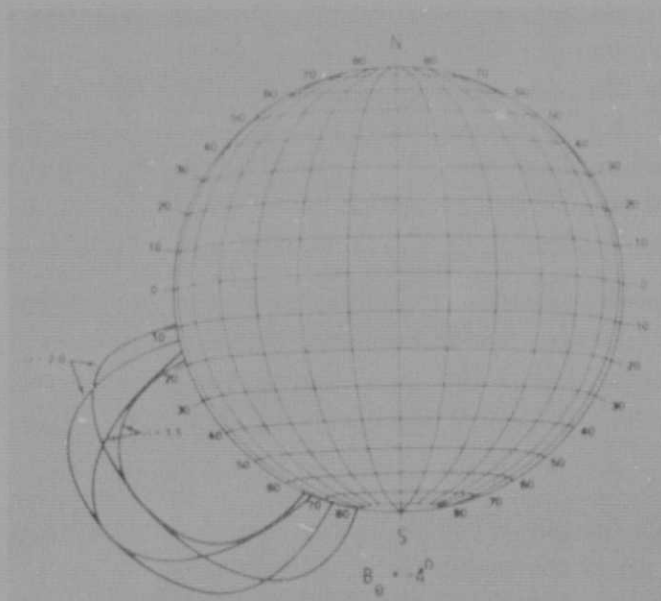
b. Selection of two values of α for each of two observed maximum heights (1.5 and 1.7 $R_\odot$); unit of α is $R_\odot^{-1}$.

Figure 5. Results of one-term (n = 2) approximation of force-free global magnetic field representation.

where μ_0 is the permeability. If $\alpha = 1.5 \, R_\odot^{-1}$, a magnetic field of 10 Gauss in the arch legs would imply current densities of 1.7×10^{-6} A m^{-2}, or currents (assuming a tube diameter of 5×10^4 km) of 3×10^9 A. Assuming a fully ionized gas with density 10^9 cm^{-3}, either an electron drift velocity of nearly equal to 1 cm s^{-1} or a net electron surplus of one part in 10^5 in a plasma flowing at 1 km s^{-1} is needed. Assuming a conductivity of 10^4 mho m^{-1} [6], Joule heating due to such currents supplies only approximately 10^{-14} ergs cm^{-3} s^{-1}, a negligible fraction of the thermal energy content.

IV. DISCUSSION

The faint nature of the arcade for the December and January limb passages rules out any temperature or density determination. However, the apparent lack of variations in intensity as well as shape for the period is striking and suggests that a condition of energy and mass equilibrium has been achieved. If the plasma, conductive flux, and wave motions are restricted to flow parallel to the direction of the magnetic field, the footpoints must be the source of energy needed to balance radiation losses within the arch. The northern foot, although not clearly defined in position, is located along the southern boundary of the active region complex (Fig. 3d) at approximately 15 degrees south. Measurements of temperatures and densities of active regions in the area indicate 3×10^6 K and 3×10^9 cm^{-3}, respectively. The southern series of arcade feet is embedded in a region of relatively little X-ray emission, probably indicating $T_e \lesssim 1.5 \times 10^6$ K and $n_e \gtrsim 10^9$ cm^{-3}. Furthermore, KPNO magnetograms show no evidence for photospheric vertical fields in the area of the southern feet to compare with those observed in the north. This seems to support the picture, as seen in X-rays, of a more confined, active northern foot, with flux tubes diverging to a weak, diffuse line of southern points.

To estimate losses due to radiation, we use cooling rates given by Cox and Tucker [7]. Since the radiation rate function $Q_R \sim \rho^2 f(T_e)$ is fairly insensitive to temperature, an isothermal flux tube at 1×10^6 K is adequate. As limits to the density distribution, we take (a) the hydrostatic case with base density $n_e = 10^9$ cm^{-3} and (b) a constant-density case, $n_e = 10^9$ cm^{-3}. We assume the shape of the tube to be semicircular of radius $0.6 \, R_\odot$; i.e., length ℓ is

1.3×10^6 km. If the cross sectional area a remains constant, the energy loss due to radiation is $1.5 \times 10^5 a$ ergs $s^{-1} < Q_R < 3.4 \times 10^6 a$ ergs s^{-1}, with the lower limit being the more realistic one.

Conductive flux, mainly from the northern foot, probably accounts for energy replenishment, although a measure of the temperature gradient over the length of the arch cannot be achieved to affirm this assumption. Indeed, if the northern leg is fed by an active region of enhanced temperature and density, the pressure difference and resulting material flow between the feet would offer an attractive alternative energy source. Very small pressure differences of perhaps $\Delta p/p \lesssim 0.01$ are sufficient to produce shocks on the descending (southern) leg [8]. However, the question of whether the density scale heights in the arch legs reflect a hydrostatic situation or a flow condition [i.e., div $(\rho u a) = 0$] cannot be definitely settled.

V. CONCLUSIONS

We have observed a large, long-lived arch structure in the corona in December 1973 and January 1974 and have found that it correlates well with a helmet streamer observed in white light. The latter observations indicate that initial evolution of the feature may have begun as early as August 1973[1] and was related to the coronal activity reported by Hildner et al. [9].

The X-ray structure showed great stability throughout the remainder of the Skylab mission, and its white-light counterpart gradually disappeared in March 1976.[2]

We suggest that the arch system owed its stability to a stable coronal magnetic-field configuration. It is possible to describe the arch system using a new global, force-free magnetic-field analysis, the elements of which have been briefly discussed.

---

1. Hansen, S.: Private Communications, 1976.

2. Ibid.

REFERENCES

1. Dunn, R. B.: Physics of the Solar Corona. C. J. Macris (ed.), Dordrecht, Holland, Reidel Publishing Co., 1971, p. 114.

2. Underwood, J. H.; Milligan, J. E.; DeLoach, A. C.; and Hoover, R. B.: The S-056 X-Ray Telescope Experiment on the Skylab-Apollo Telescope Mount. Applied Optics, vol. 16, 1977 (in press).

3. Vaiana, G. S.; Krieger, A. S.; Petrasso, R.; Silk, J. K.; and Timothy, A. F.: Instrumentation in Astronomy — II. L. Larmore and D. Crawford (eds.), Seminar Proceedings, Society of Photo-Optical Instrumentation Engineers, vol. 44, 1974, p. 185.

4. Chase, R. G.; Krieger, A. S.; Svestka, Z.; and Vaiana, G. S.: X-Ray Loops Connecting Separate Active Regions. Eighteenth Plenary Meeting of COSPAR, Varna, Bulgaria, May 29-June 7, 1975.

5. Nakagawa, Y.; Wu, S. T.; and Tandberg-Hanssen, E.: Private Communication. Presently in preparation for publication in the open literature.

6. Heyvaerts, J.: Solar Physics, vol. 38, 1974, p. 419.

7. Cox, D. P. and Tucker, W. H.: Ap. J., vol. 157, 1969, p. 1157.

8. Meyer, F.: Physics of the Solar Corona. C. J. Macris (ed.), Dordrecht, Holland, Reidel Publishing Co., 1971, p. 29.

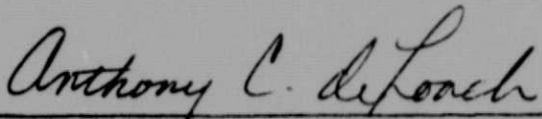9. Hildner, E.; Gosling, J. T.; and Hansen, R. T.: Solar Physics, vol. 45, 1975, pp. 363-376.

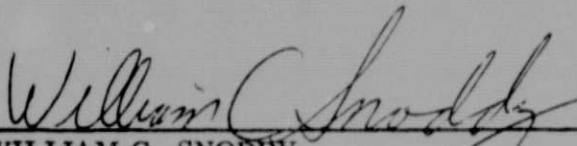# APPROVAL

A LONG-LIVED CORONAL X-RAY ARCADE

By J. P. McGuire, E. Tandberg-Hanssen, K. R. Krall,
S. T. Wu, J. B. Smith, Jr., and D. M. Speich

The information in this report has been reviewed for security classi-
fication. Review of any information concerning Department of Defense or
Atomic Energy Commission programs has been made by the MSFC Security
Classification Officer. This report, in its entirety, has been determined to
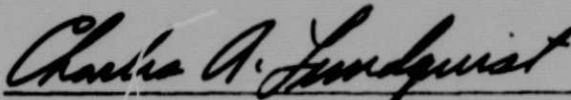be unclassified.

This document has also been reviewed and approved for technical
accuracy.

ANTHONY C. DeLOACH
Chief, Solar Sciences Branch

WILLIAM C. SNODDY
Chief, Solar-Terrestrial Physics Division

CHARLES A. LUNDQUIST
Director, Space Sciences Laboratory